0.010 cm^3/g) was estimated by Kwok (*7*) from the amino acid composition. For the molecular weight, we adopt the most commonly reported value (*8*) and assign to it a generous error (M = 560,000 ± 25,000). With these estimates we find that n is 6.3 ± 0.5. If the estimates of errors in all quantities are doubled, the resulting error is ± 0.8. If the estimated error in molecular weight is doubled and all other errors quadrupled, n = 6.3 ± 1.2. Thus it is unlikely that there are eight molecules per cell and very unlikely that there are four.

The evidence for six molecules per unit cell, rather than two, four, or eight, is supported by intensities of reflections on the $h0l$ zone of the x-ray pattern. Along the 0,0,l line [c-axis (*9*)], the 0,0,3; 0,0,6; and 0,0,12 reflections are strong, but the 0,0,4 reflection is weak. This implies that, at very low resolution, the structure when viewed along the a- or b-axis is composed of three layers of electron-dense material (RuBPCase molecules). Moreover, the exceedingly strong 0,0,6 reflection is consistent with the notion that each molecule is itself a double-layered structure (see below). A unit cell with two or four layers of molecules is not compatible with these intensities, nor are such cells consistent with the c-axial dimension (which is roughly three times the observed molecular diameter of 115 Å) (*4*).

By combining information from both the form I and form II crystals, we can determine the symmetry of the RuBPCase molecule. Our study of form I crystals (*4*) showed that RuBPCase molecules have a minimum symmetry of three mutually perpendicular twofold axes (D_2 = 222). Similarly, the six molecules per unit cell in the form II crystals, must occupy special positions of defined symmetry. Two of the molecules contain at least a fourfold axis of rotation, and the remaining four contain at least a twofold axis. If we assume that all molecules are identical, then the combined symmetries of D_2 (222) and C_4 (*4*) in the two crystal forms demand that the RuBPCase molecule has D_4 (422) symmetry. This is the highest symmetry that an L_8S_8 oligomer can possess, and it is the symmetry expected for a self-assembling aggregate of this stoichiometry.

The filtered reconstruction of Fig. 3 contains some additional information on subunit structure. Each molecule in the filtered images (Fig. 3, b and c) is averaged with ~ 24 equivalent neighboring molecules. The filtered molecules are squarish in outline and appear to contain a fourfold rotation axis coincident with the hole. Four elliptical units appear bonded in a square planar ring with four faint spikes of density (arrow, Fig. 3b) at the intersections of denser units. The filtering procedure has slightly enhanced the presence of the molecules obscured by stain (Fig. 3c).

From these filtered images and from the molecular symmetry, we propose a model of RuBPCase quaternary structure: the molecule is double layered, with each layer comprised of a ring of four large, elliptical subunits. The two layers are nearly eclipsed as suggested by the images in electron micrographs, even though this is not required by symmetry. The spikes at the corners of the square molecules (arrow, Fig. 3b) may conceivably be the small subunits, or the spikes may result from the superposition of parts of the obscured molecules with the clear molecules. Figure 4 depicts this model schematically, showing the arrangement of molecules in the form II crystals.

TIMOTHY S. BAKER
DAVID EISENBERG
FREDERICK EISERLING

Departments of Chemistry and Bacteriology and Molecular Biology Institute, University of California, Los Angeles 90024

References and Notes

1. S. G. Wildman, K. Chen, J. C. Gray, S. D. Kung, P. Kwanyuen, K. Sakano, in *Genetics and Biogenesis of Chloroplasts and Mitochondria*, P. S. Perlman, C. W. Birky, T. J. Byers, Eds. (Ohio State Univ. Press, Columbus, 1975), chap. 9; I. Takebe and Y. Otsuki, *Planta* **113**, 21 (1973); B. E. S. Gunning, M. W. Steer, M. P. Cochrane, *J. Cell Sci.* **3**, 445 (1968); M. Wrischer, *ibid.* **75**, 309 (1967); C. Larsson, C. Collin, P. A. Albertsson, *J. Ultrastruct. Res.* **45**, 50 (1973).
2. L. K. Shumway, T. E. Weier, C. R. Stocking, *Planta* **76**, 182 (1967).
3. P. J. Chan, K. Sakano, S. Singh, S. G. Wildman, *Science* **176**, 1145 (1972); R. Chollet, L. L. Anderson, L. C. Hovespian, *Plant Physiol.* **56** (Suppl.), 26 (1975).
4. T. S. Baker, D. Eisenberg, F. A. Eiserling, L. Weissman, *J. Mol. Biol.* **91**, 391 (1975).
5. N. F. M. Henry and K. Lonsdale, in *International Tables for X-ray Crystallography* (Kynock, Birmingham, England, ed. 3, 1969), vol. 1, p. 180.
6. B. W. Low and F. M. Richards, *J. Am. Chem. Soc.* **76**, 2511 (1954).
7. S. Y. Kwok, thesis, University of California, Los Angeles (1972).
8. M. I. Siegel, M. Wishnick, M. D. Lane, in *The Enzymes*, P. D. Boyer, Ed. (Academic Press, New York, ed. 3, 1972), vol. 6, pp. 169–192.
9. In the proposed packing, these single "defect" molecules should appear with the same brightness as the "obscured" molecules. In fact they are brighter. This could arise from any of the following: (i) A nonintegral number of unit cells in this platelet; (ii) uneven wetting of stain (for example, the defect molecules could simply be normal molecules with a bit of dried stain on top); or (iii) unequal affinity of stain for the crystallographically nonequivalent positions occupied by "obscured" and "defect" molecules.
10. We acknowledge with thanks support from PHS, NSF, and the Research Corporation, and also the help of K. Chen in obtaining pure enzyme.

13 July 1976; revised 12 November 1976

High Rates of Vertical Crustal Movement near Ventura, California

Abstract. *Fission track, radiometric, and paleomagnetic age determinations in marine sedimentary rocks of the Ventura Basin make it possible to estimate the vertical components of displacement rates for the last 2 million years. The basin subsided at rates up to 9.5 ± 2.5 millimeters per year until about 0.6 million years ago, when subsidence virtually ceased. Since then, the northern margin of the basin has been rising at an average rate of 10 ± 2 millimeters per year, about the same rate as that based on the geodetic record north and west of Ventura since 1960 but considerably lower than the rate along the San Andreas fault at Palmdale since 1960.*

The Ventura Basin has long been known for its thick sedimentary sequence of late Cenozoic age, which was strongly deformed during the Pleistocene (*1*). This sequence consists of deep-water sandstones and siltstones of the Fernando Formation overlain conformably by the shallow-marine and nonmarine Saugus Formation, which is itself overlain unconformably by alluvial deposits including the Mugu and Oxnard aquifers. The marine part of this sequence is highly fossiliferous, but the provinciality of the fossil assemblages precludes precise correlation with worldwide Cenozoic stages calibrated in radiometric ages. Recently, however, the Bailey ash bed midway in the Fernando-Saugus sequence was dated as 1.2 ± 0.2 million years by the fission-track method on zircon (*2*), and paleomagnetic stratigraphy of the Saticoy oil field was used to identify the Olduvai and Jaramillo normal events of the Matuyama reversed epoch (*3*). Constraints on the minimum age of the Saugus Formation are provided by the ages of two biostratigraphically distinct sets of marine terraces along the California coast as determined by uranium-series methods (*4*) and amino acid racemization (*5*); these ages are 0.09 and 0.13 million years, respectively, with a considerable margin of error. A similar but undated set of marine terraces north and west of the city of Ventura truncates the south-dipping Saugus Formation (*6*). Uplift rates in the Santa Monica Mountains based on the dated terraces there led

Birkeland (*7*) to estimate by extrapolation the age of an older, higher terrace in the Santa Monica Mountains as 0.25 million years.

Because the Ventura Basin is a major oil-producing region, it has been possible to supplement the data from surface geology with data from over 2000 logs from oil and water wells to construct a three-dimensional stratigraphic and structural geologic framework; this framework is described elsewhere (*8*). Figure 1 shows three stratigraphic sections from the central Ventura Basin. Section A–A′ follows the deep axis of the basin north of the Oak Ridge fault, section B–B′ is parallel to section A–A′ but south of the fault, and section C–C′ cuts across the structural grain from the eroded northern margin of the basin across the Oak Ridge fault and Oxnard plain to the southern margin of the basin. Much of the Santa Clara Valley and Oxnard plain has not undergone any significant amount of erosion since the Saugus Formation was deposited; it is at maximum depth of burial today. Where the section is now at maximum burial, the present depositional surface is used as the stratigraphic datum; elsewhere, microfaunal horizons within the Fernando Formation are used (*9*). The vertical bar at Saticoy in section A–A′ shows the magnetic reversal stratigraphy determined by Blackie and Yeats (*3*), and sections B–B′ and C–C′ show the position of the Bailey ash which was dated by the fission-track method. If the Olduvai event is considered to be near the Plio-Pleistocene boundary, correlation of this boundary on section A–A′ from Saticoy east to Bardsdale indicates that, at Bardsdale, the Quaternary sequence alone is nearly 5 km thick. This may be the thickest Quaternary sequence in the world.

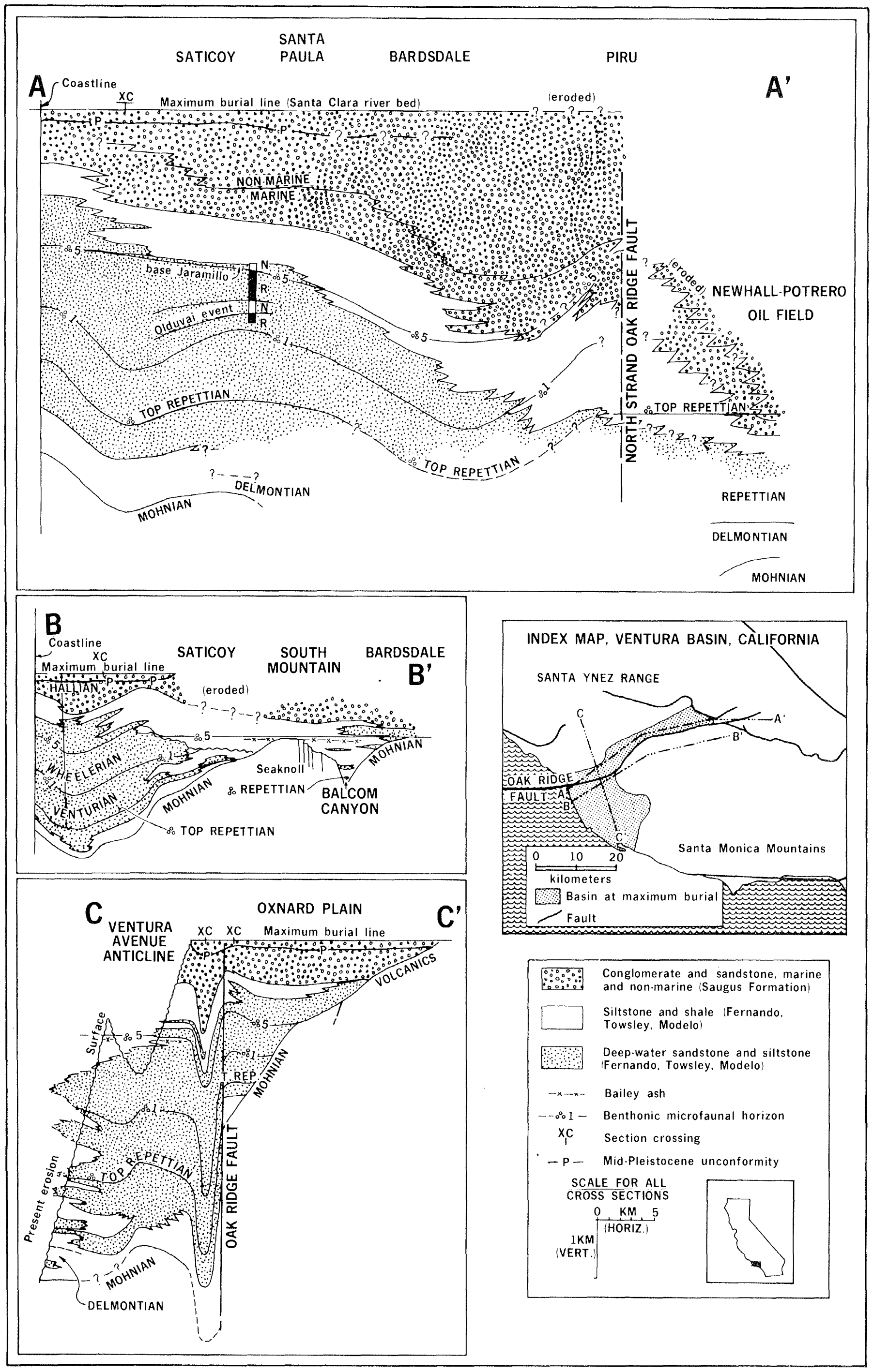

Fig. 1. Stratigraphic sections across the central trough of the Ventura Basin (vertical exaggeration, × 5). The maximum burial line is used as the datum where the section is now at maximum burial; elsewhere, a Fernando microfaunal marker (⁂ 5 or Top Repettian) is selected as the datum. Section *A–A′* follows the deepest part of syncline north of the Oak Ridge fault; the vertical bar at Saticoy shows the magnetic reversal stratigraphy of the Saticoy oil field (*3*) correlated by microfauna and subsurface stratigraphy to the adjacent syncline. The distribution of Bailey ash shown on sections *B–B′* and *C–C′* is based on surface mapping (*16*), which shows the ash to underlie microfaunal marker ⁂ 5. Section *B–B′* is immediately across the Oak Ridge fault from section *A–A′*; the thinner section is due to movement on the Oak Ridge fault during sedimentation. Stratigraphic sections at the coastline and Bardsdale in sections *A–A′* and *B–B′* were used to determine displacement rates in Fig. 2 and Table 1. For correlations of Mohnian, Delmontian, Repettian, Venturian, Wheelerian, and Hallian provincial stages with Cenozoic epochs, see (*9*) and (*10*).

Figure 2 and Table 1 show vertical crustal displacement rates based on the thickness of several sequences adjacent to the Oak Ridge fault and shown in Fig. 1. These rates are calibrated in terms of the Olduvai event, the fission-track age of the Bailey ash, and the base of the Jaramillo event. The constraints of marine terrace ages lead to a rough estimate of the age of the end of Saugus deposition near the coast of 0.6 ± 0.1 million years. Presumably, 0.6 million years is the age of the mid-Pleistocene unconformity shown in Fig. 1; younger sediments in the Santa Clara Valley and Oxnard plain may have been deposited during the time much of the rest of the basin was being uplifted. An additional constraint is a fission-track zircon age of 6.8 million years from an ash bed in the Mohnian (*10*) sequence at Balcom Canyon (*11*).

Sediment accumulation rates used in Table 1 do not take into account the effects of compaction, as described by McCulloh (*12*), nor do they account for changes in water depth at the time of sedimentation from 2000 m in the Repettian to sea level in the Saugus, as described by Natland (*9*). Because water depths in beds of the same age in the Fernando and Saugus formations were the same on both sides of the Oak Ridge fault, a consideration of water depth would not affect the value of the vertical component of displacement rates across this fault. In general, rates of sediment accumulation are higher in the range $0.6 \lesssim t \lesssim 1$ million years than in the range $1 \lesssim t \lesssim 2$ million years. If the rates for $t \gtrsim 2$ million years are assumed to be the same as those in the range $1 \lesssim t \lesssim 2$ million years, the age of the provincial Miocene-Pliocene boundary based on an extrapolation down-section of these rates is 4 million years, as compared with the 5-million-year age of the Miocene-Pliocene boundary elsewhere in the world. This extrapolated age is lower than the fission-track age of the late Miocene ash bed at Balcom Canyon.

Table 1. Rates of vertical crustal displacement (in millimeters per year) adjacent to the Oak Ridge fault, Ventura Basin. Negative values represent subsidence; positive values, uplift. Slip rates on the Oak Ridge fault are in absolute values and represent the vertical component only.

Displacement or slip rate	Time range (million years)		
	$0 \lesssim t \lesssim 0.6$	$0.6 \lesssim t \lesssim 1$	$1 \lesssim t \lesssim 2$
	Ventura coast		
North of fault	−0.3	−5.8	−1.4
South of fault	−0.2	−2.5	−0.7
Slip rate on fault	0.1	3.3	0.7
	Bardsdale area		
North of fault	−0.7	−8.9	−1.3
South of fault	+2.5 to +4	−1.3 to −2.8	0
Slip rate on fault	3.2 to 4.7	6.1 to 7.6	1.3

Vertical displacement rates near the coast are negative because both sides of the Oak Ridge fault went down during the time of deposition of the Fernando and Saugus formations and are now at maximum burial. Farther inland, at Bardsdale, the positive values south of the fault in the range $0 \lesssim t \lesssim 0.6$ million years reflect late Quaternary uplift, and the range of values reflects uncertainty about the total thickness of Saugus Formation deposited there and subsequently eroded away. The uplift there is estimated as 1.5 to 2.4 km, as based on the estimated thickness of beds formerly overlying nonmarine Oligocene strata now exposed at the surface. The rate of sediment accumulation at Bardsdale, north of the fault, was nearly 9 mm/year in the range $0.6 \lesssim t \lesssim 1$ million years, possibly the highest long-term sediment accumulation rate known. The vertical component of movement on the Oak Ridge fault shows a fourfold increase in both areas about 1 million years ago (Fig. 2; Table 1). At Bardsdale, fault motion has continued at a high rate for the last 0.6 million years, but near the coast fault motion decreased by at least an order of magnitude.

The uplift at Bardsdale (1.5 to 2.4 km) is small compared to that at the northern rim of the Ventura Basin. As shown in section C–C′, about 6 km of section have been removed in the last 0.6 million years, if the maximum burial line near the coast is extrapolated to the northern rim of the basin. It is quite possible that the original thickness of the Fernando and Saugus formations now eroded away was less than the thickness of these formations now preserved, but this would not reduce the thickness of the eroded section by more than 1 km. Because the late Cenozoic depositional cycle under discussion began with the Delmontian (*8*, *10*), I assumed in arriving at the figure of 6 km that the removal of rocks with a Delmontian fauna, along with the younger Fernando and Saugus formations, took place entirely in the last 0.6 million years. Undoubtedly some of the underlying Mohnian was also removed during this time, but the presence of clasts with Mohnian fossils in the Fernando Formation indicates that part of the erosion of Mohnian beds took place earlier than 0.6 million years ago. Thus the figure of 6 ± 1 km appears to be the best approximation. On the basis of this figure, the uplift rate is calculated as 10 ± 2 mm/year.

The high rate of subsidence north of the fault at Bardsdale and the high rate of uplift of the northern rim of the basin place constraints on the age of the end of Saugus deposition, because subsidence of one area preceded uplift of the other. If the age of the end of deposition is taken as 0.7 million years, instead of 0.6 million years, the subsidence rate at Bardsdale increases to 12 mm/year and the uplift of the northern rim decreases to 8.6 mm/year. If deposition ended 0.5 million years ago, the subsidence rate at Bardsdale is 7.1 mm/year but the rate of uplift of the northern rim is 12 ± 2 mm/year. It is clear that this age could not be much younger than 0.5 million years or much older than 0.7 million years, because the vertical movement rates at either extreme would be unreasonably high.

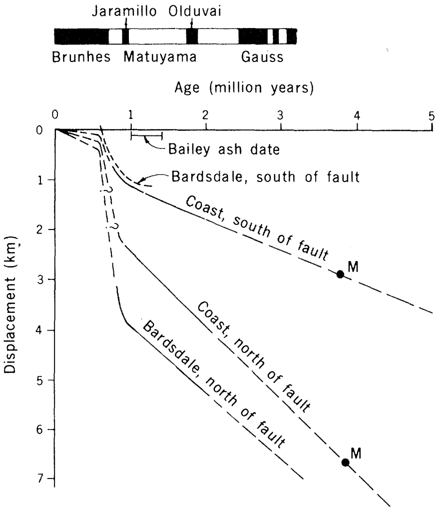

Fig. 2. Rates of vertical crustal displacement at four localities in the Ventura Basin adjacent to the Oak Ridge fault. Age controls are the Olduvai event and the base of the Jaramillo event, identified in the Saticoy oil field (*3*) and correlated to each locality, the Bailey ash bed (*2*), and the end of deposition, constrained by uranium-series (*4*) and amino acid racemization (*5*) ages of marine terraces. *M* is top of provincial California Miocene in two coastal sections.

It is possible to compare the average rate of uplift in the last 0.6 million years to uplift rates in historic times. Uplift rates based on erosion and sediment yields in mountain watersheds of the Transverse Ranges for periods of 25 to 42 years are as high as 2.3 mm/year (*13*). The geodetic record indicates that uplift since 1934 in the Santa Ynez Range north of section C–C′ is broad and uniform with a hinge line near the Red Mountain fault at the northern margin of the basin; uplift rates are 2 to 5 mm/year from 1934 to 1960 and 6 to 9 mm/year from 1960 to 1968 (*14*). This uplift is in the southwestern part of a broad bulge trending east-west and centering on the San Andreas fault at the town of Palmdale, where over the last 15 years uplift has been occurring at rates as high as 16.7 mm/year (*14*, *15*). Uplift rates in the mountains north of Ventura over the last 0.6 million years are about equal to rates in that area since 1960 but considerably lower than the rates at Palmdale since 1960.

ROBERT S. YEATS
Department of Geology,
Ohio University, Athens 45701

References and Notes

1. R. D. Reed and J. S. Hollister, *Structural Evolution of Southern California* (American Association of Petroleum Geologists, Tulsa, Okla., 1936); T. L. Bailey, *Geol. Soc. Am. Bull.* **54**, 1549 (1943).
2. G. A. Izett, C. W. Naeser, J. D. Obradovich, *Geol. Soc. Am. Abstr. Programs* **6**, 197 (1974).
3. G. W. Blackie and R. S. Yeats, *Am. Assoc. Petrol. Geol. Bull.* **60**, 1985 (1976).
4. B. J. Szabo and J. N. Rosholt, *J. Geophys. Res.* **74**, 3253 (1969); J. W. Valentine and H. H. Veeh, *Geol. Soc. Am. Bull.* **80**, 1415 (1969).

5. J. Wehmiller, E. Peterson, K. Kvenvolden, K. Lajoie, R. Wright, *Eos* **56**, 1139 (1974); K. Lajoie, J. Wehmiller, K. Kvenvolden, E. Peterson, R. Wright, *Geol. Soc. Am. Abstr. Programs* **7**, 338 (1975).
6. W. C. Putnam, *Geol. Soc. Am. Bull.* **53**, 691 (1942).
7. P. W. Birkeland, *J. Geol.* **80**, 432 (1972).
8. H. E. Nagle and E. S. Parker, in *Future Petroleum Provinces of the United States—Their Geology and Potential*, I. H. Cram, Ed. (Memoir 15, American Association of Petroleum Geologists, Tulsa, Oklahoma, 1971), p. 254; R. S. Yeats, in *The Neogene Symposium*, A. E. Fritsche, H. Ter Best, Jr., W. W. Wornardt, Eds. (Pacific Section, Society of Economic Paleontologists and Mineralogists, San Francisco, Calif., 1976), p. 19; M. M. Mukae and J. M. Turner, "Ventura County water resources management study: geologic formations, structures and history in the Santa Clara–Calleguas area" (Ventura County Department of Public Works, Technical Information Record, Ventura, Calif., 1975).
9. These microfaunal horizons, described by M. L. Natland [thesis, University of California at Los Angeles (1952)], are based on benthonic foraminifera which are controlled by water depths rather than evolutionary changes in fauna. The terms Repettian, Venturian, Wheelerian, and Hallian, as used in Fig. 1, are microfaunal stages erected by Natland. However, within a single restricted environment, the abyssal plain, they may approach time lines and are so used in Fig. 1. In this environment in the Ventura Basin, the Repettian stage is early Pliocene, the Venturian late Pliocene, the Wheelerian Plio-Pleistocene, and the Hallian early Pleistocene in age. The water depth shoals from about 2000 m in the Repettian to 400 m near microfaunal horizon 5 where it is within the deep-water sandstone sequence; the water depth is unrelated to the sedimentation rate within the region covered by Fig. 1.
10. Mohnian and Delmontian are names of microfaunal stages erected by R. M. Kleinpell, *Miocene Stratigraphy of California* (American Association of Petroleum Geologists, Tulsa, Oklahoma, 1938). The Mohnian is late Miocene and the Delmontian is latest Miocene–earliest Pliocene in age.
11. C. W. Naeser and J. D. Obradovich, personal communication.
12. T. H. McCulloh, *U.S. Geol. Surv. Prof. Pap. 528-A* (1967).
13. K. M. Scott and R. P. Williams. *U.S. Geol. Surv. Water-Resourc. Invest. 47-73* (1974).
14. J. M. Buchanan-Banks, R. O. Castle, J. I. Ziony, *Tectonophysics* **29**, 113 (1975). Calculated values are based on figure 2 of this paper.
15. R. O. Castle, J. P. Church, M. R. Elliott, *Science* **192**, 251 (1976); ——, N. L. Morrison, *Tectonophysics* **29**, 127 (1975).
16. R. S. Yeats and W. A. McLaughlin, *Geol. Soc. Am. Spec. Pap. 124* (1970), p. 173.

17. I thank the oil companies operating in the Ventura Basin for their release of proprietary well data, and J. D. Obradovich, A. Sarna-Wojcicki, and J. C. Taylor for critical review of the manuscript. This work was supported by National Science Foundation Geophysics Section grant GA 36035 and U.S. Geological Survey contracts 14-08-0001-15271 and 14-08-0001-15886.

6 August 1976; revised 27 October 1976

Hydrogen Peroxide Induces Spawning in Mollusks, with Activation of Prostaglandin Endoperoxide Synthetase

Abstract. *Addition of hydrogen peroxide to seawater causes synchronous spawning in gravid male and female abalones, and certain other mollusks as well. This effect is blocked by exposure of the animals to aspirin, an inhibitor of the enzyme catalyzing oxidative synthesis of prostaglandin endoperoxide. Hydrogen peroxide activates this enzymatic reaction in cell-free extracts prepared from abalone eggs (a very rich source of the prostaglandin endoperoxide synthetase); this effect appears to reveal a fundamental property of prostaglandin endoperoxide synthesis. Applicability of these findings to both mariculture and medical purposes is suggested.*

Although the marine invertebrate animals constitute a vast and protein-rich food resource, control of their reproduction remains one of the principal barriers to their economical cultivation for human consumption (*1*). Accordingly, we have begun to investigate chemical means for controlling the reproduction and early development of the abalone, a large herbivorous marine snail (molluscan gastropod) valued as a highly palatable source of meat protein in parts of the United States, Mexico, Australia, Africa, China, and Japan. We have found that the addition of hydrogen peroxide to seawater causes gravid male and female abalones (as well as certain other mollusks) to spawn, and that this effect may result from a direct activation of the enzyme-catalyzed synthesis of prostaglandin endoperoxide.

Experiments described here were performed with *Haliotis rufescens*, the red abalone, as gravid specimens may be found throughout the year (*2*); this is also the species of principal importance to the commercial fishery in the United States. These bottom-dwelling animals reproduce by broadcast spawning, with synchronous and copious liberation of gametes from animals of both sexes resulting in external fertilization and the subsequent development of free-swimming planktonic larvae (*3, 4*).

Spawn liberated from abalones of either sex can trigger responsive spawning in animals of the opposite sex (*3, 5*). We have found that this response can be detected with sensitivity and specificity by testing animals singly at 13° to 14°C, at which the spontaneous spawning of gravid animals is effectively suppressed (Table 1, section 1).

Under these conditions, we have tested compounds known to affect reproduction in other species (Table 1, section 2). Prostaglandin E and prostaglandin F [both known to mediate various physiological reactions, which in turn regulate ovulation, fertilization, pregnancy, and birth in humans and other species (*6*)] are occasionally effective in inducing spawning in both male and female abalones, under conditions in which comparably gravid animals, receiving control treatment in parallel, fail to spawn. Specificity of this effect is indicated by the failure of both mammalian gonadotropin and thyroxin [the latter capable of inducing spawning in male oysters (*7*)] to elicit any detectable response under these conditions.

The biosynthesis of prostaglandins is known to depend on the prior synthesis of prostaglandin endoperoxides; these unique, short-lived intermediates contain both unusual endoperoxide and hydroperoxy moieties, sequentially introduced from molecular oxygen by the catalytic activity of the enzyme fatty acid cyclooxygenase (prostaglandin endoperoxide synthetase) (*8*). Prostaglandin endoperoxides are the direct precursors of both the prostaglandins and the physiologically potent thromboxanes; the endoperoxides themselves may also be physiologically active (*8–10*). We were thus interested in investigating possible effects resulting from direct addition of the uniquely reactive oxidant hydrogen peroxide (H_2O_2) to seawater containing gravid abalones.

Addition of H_2O_2 (to a concentration of ~ 5 m*M* in alkaline seawater, *p*H ~ 9.1) reproducibly causes spawning in both male and female abalones within 3 ± ½ hours after the first addition (Fig. 1 and Table 1, section 3). This induction can be blocked by aspirin, added to the seawater 15 minutes before the H_2O_2. Aspirin (acetylsalicylic acid) is a well-characterized inhibitor of the fatty acid cyclooxygenase-catalyzed first step in the conversion of arachidonic acid to prostaglandin endoperoxide (*10, 11*). The inhibition of the H_2O_2 induction of spawning by aspirin suggests, then, that cyclooxygenase activity and prostaglandin endoperoxide synthesis may be required in the animal during its exposure to H_2O_2 for the induction of spawning.

Rapid and specific extracellular destruction of H_2O_2 by catalase, added to seawater before the peroxide, also effectively blocks the induction of spawning (Table 1, section 3), which proves that it is the H_2O_2 molecule itself (rather than some contaminant) that is responsible for this induction. Blockade by the generalized reducing agent mercaptoethanol is consistent with the hypothesis that the action of H_2O_2 responsible for the induction of spawning is essentially an oxidative one. In fact, we have found that oxygen gas, bubbled through seawater containing gravid abalones, is marginally